

# Zn(II) and Cd(II) Coordination Polymers with an *N,O*-Donor Ligand: Structural Characterization and Fluorescence Properties

Hai-Wei Kuai, Xiao-Chun Cheng and Xiao-Hong Zhu

Faculty of Life Science and Chemical Engineering, Huaiyin Institute of Technology, Huaian 223003, P. R. China

Reprint requests to Dr. Hai-Wei Kuai. Fax: +86-517-83559216. E-mail: [hyitshy@126.com](mailto:hyitshy@126.com)

*Z. Naturforsch.* **2013**, 68b, 789–796 / DOI: 10.5560/ZNB.2013-3094

Received March 3, 2013

The hydrothermal reactions of 5-(benzimidazol-1-ylmethyl)isophthalic acid ( $H_2L$ ) with Zn(II) and Cd(II) salts lead to the formation of the two new complexes [Cd(L)] (**1**) and [Zn(L)] (**2**). In the presence of 2-(pyridin-2-yl)-1*H*-benzimidazole (pybim) as auxiliary ligand, complex [Zn(L)(pybim)] (**3**) was obtained. Complexes **1–3** have been characterized by single-crystal and powder X-ray diffraction, IR spectroscopy, and elemental and thermogravimetric analyses. Complexes **1** and **2** are isostructural and exhibit a binodal (3,6)-connected 2D **kgd** network structure with  $(4^3)_2(4^6.6^6.8^3)$  topology; **3** consists of uninodal 3-connected 2D ( $6^3$ ) **hcb** networks. The influential factors of synthetic strategies on the coordination modes of the ligands and on the structures and properties of the resulting complexes are discussed. The luminescence properties of **1–3** were investigated.

*Key words:* Zn(II), Cd(II), Metal-Organic Frameworks, Fluorescence and Thermal Decay

## Introduction

In the past decade, much progress has been achieved in the synthesis and structural characterization of metal-organic frameworks (MOFs), many of which exhibit fascinating structures, interesting properties, and potential applications in many fields [1–4]. Current efforts have been focused on the exploration of such inorganic-organic hybrid materials with multifunctional properties, such as catalytic, absorptive, magnetic, and electric properties, and of fluorescence and nonlinear optical (NLO) effects [5–8]. The functional properties of complexes are closely related to the nature of the metal centers and of the ligands, and their architectures. For example, complexes containing metal centers with  $d^{10}$  electron configuration, such as Zn(II) and Cd(II), may exhibit luminescence [9, 10]; metal ions possessing unpaired electrons, such as Mn(II), Co(II), Ni(II), and Cu(II) can be bridged by ligands to form polynuclear subunits which mediated magnetic interactions [11–13]; when complexes crystallize in an acentric space group, induced by a dipolar ligand such as 4-(pyridin-4-yl)benzotrile, then non-centrosymmetric structures may show second-order

non-linear optical (NLO) effects [14]. Therefore, it becomes significant to assemble complexes under different synthetic conditions, which can give access to composite polymers with novel functional properties in the vast domain of multifunctional materials.

For the construction of MOFs [15–17], multi-dentate organic ligands with *N*- or *O*-donors are often utilized as building blocks; for example, multicarboxylate ligands are suitable to build polymers due to their versatile coordination modes and structural diversity. Imidazole-, pyridine-, or benzimidazole-containing *N*-donors can react with various metal salts leading also to the formation of MOFs with multi-dimensional architectures and interesting functional properties [18–21]. Recent studies have further demonstrated that mixed organic ligands, especially mixed *N,O*-donor ligands, are good candidates for the construction of novel MOFs due to tunable factors [22–24]. Following such synthetic strategy, we have been focusing our attention on coordination reactions of 5-(benzimidazol-1-ylmethyl)isophthalic acid ( $H_2L$ ) with various metal salts. The  $H_2L$  ligand is an efficient and versatile organic building unit already used in our previous studies, exhibiting an advantage

over other *N*- or *O*-donor ligands since it possesses both carboxylate and flexible benzimidazol-1-ylmethyl groups. Hitherto, two copper complexes showing NLO effects and two manganese and two cobalt complexes with interesting magnetic properties have already been reported [25, 26]. From a continuation of our research, we report herein the synthesis and structural characterization of three luminescent coordination polymers [Cd(L)] (**1**), [Zn(L)] (**2**) and [Zn(L)(pybim)] (**3**) [pybim = 2-(pyridin-2-yl)-1*H*-benzimidazole]. The fluorescence and the decomposition of **1–3** were also examined.

## Results and Discussion

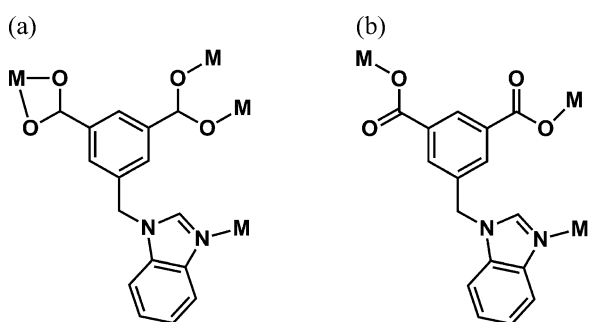
### Preparation

The hydrothermal reactions of stoichiometric amounts of Cd(II) and Zn(II) salts with H<sub>2</sub>L provided single-crystalline materials of **1** and **2**. When pybim was introduced into the zinc salt reaction system as auxiliary ligand, complex **3** was obtained. Complexes **1–3** are stable in air. The crystal structures of **1–3** are discussed in detail in the following sections.

### Structural description of [Cd(L)] (**1**) and [Zn(L)] (**2**)

The same space group and similar cell parameters as listed in Table 1 imply that complexes **1** and **2** are isostructural, and the results of the structure analyses indicate that they have the same 2D network structure. Therefore, only the structure of **1** is described in detail here.

Complex **1** crystallizes in the monoclinic system with space group *P2*<sub>1</sub>/*c*. Its asymmetric unit consists



Scheme 1. Coordination modes of the L<sup>2-</sup> ligand in the complexes: A in **1** and **2**; B in **3**.

of one Cd<sup>2+</sup> cation and one L<sup>2-</sup> anion. As shown in Fig. 1a, each Cd atom is five-coordinated by one benzimidazolyl N atom and four carboxylate O atoms from three different L<sup>2-</sup> ligands to furnish a distorted square-pyramidal coordination geometry [CdNO<sub>4</sub>]. The best equatorial plane is defined by the O1, O2, O3, and O4 atoms [mean deviation 0.214 Å], and the metal deviates by 0.503 Å from the mean plane toward N1. The Cd–N/O bond lengths vary from 2.1979(16) to 2.3211(18) Å, and the bond angles are in the range from 56.31(6) to 156.27(7)°, comparable to previously reported values for Cd(II) complexes. One carboxylate group adopts a μ<sub>1</sub>-η<sup>1</sup>:η<sup>1</sup>-chelating coordination mode, the other is μ<sub>2</sub>-η<sup>1</sup>:η<sup>1</sup>-bridging with almost identical C–O bond lengths [1.255(3) and 1.248(3) Å]. The two corresponding Cd–O bond lengths are almost identical [2.3211(18) and 2.3052(19) Å]. In complex **1**, two Cd(II) atoms are bridged by a μ<sub>2</sub>-η<sup>1</sup>:η<sup>1</sup> carboxylate group (Scheme 1, A) to form a binuclear secondary building unit (SBU) [Cd<sub>2</sub>(COO)<sub>2</sub>] with a Cd···Cd distance of 3.92 Å, which is shorter than the sum of two van der Waals radii (4.60 Å). Each SBU is connected to six adjacent ones through L<sup>2-</sup> ligands to form a 2D network structure perpendicular to the *a* axis (Fig. 1b). Using topology to analyze the structure, each SBU could be regarded as a 6-connector node, and the L<sup>2-</sup> ligand as a 3-connector node, and thus, the resultant structure of **1** could be simplified as a binodal (3,6)-connected 2D **kgd** network with (4<sup>3</sup>)<sub>2</sub>(4<sup>6</sup>.6<sup>6</sup>.8<sup>3</sup>) topology (Fig. 1c) [27].

### Structural description of [Zn(L)(pybim)] (**3**)

Complex **3** also crystallizes in the monoclinic space group *P2*<sub>1</sub>/*c*. The asymmetric unit of **3** contains one Zn<sup>2+</sup> cation, one L<sup>2-</sup> anion, and one pybim molecule. Each Zn atom is fourfold coordinated with tetrahedral coordination geometry [N<sub>2</sub>O<sub>2</sub>] by two carboxylate oxygen atoms from two different L<sup>2-</sup> ligands and two nitrogen atoms from a pybim molecule and a benzimidazolyl group (Fig. 2a). The coordinating bond lengths vary from 1.983(2) to 2.059(3) Å, the bond angles are in the range from 99.81(12) to 133.35(12)°, comparable to previously reported values for Zn(II) complexes. Both carboxylate groups in the L<sup>2-</sup> ligand of complex **3** show a μ<sub>1</sub>-η<sup>1</sup>:η<sup>0</sup>-monodentate coordination mode. Each L<sup>2-</sup> ligand bridges three different Zn atoms, and in turn each Zn(II) atom is coordinated by three different L<sup>2-</sup> ligands. These connections extend infinitely to

form a 2D network (Fig. 2b). Both the  $L^{2-}$  ligands and the Zn(II) atoms in **3** can be regarded as 3-connectors, and thus, the network of **3** can be simplified into a uninodal 3-connected 2D **hcb** network with  $(6^3)$  topology (Fig. 2c).

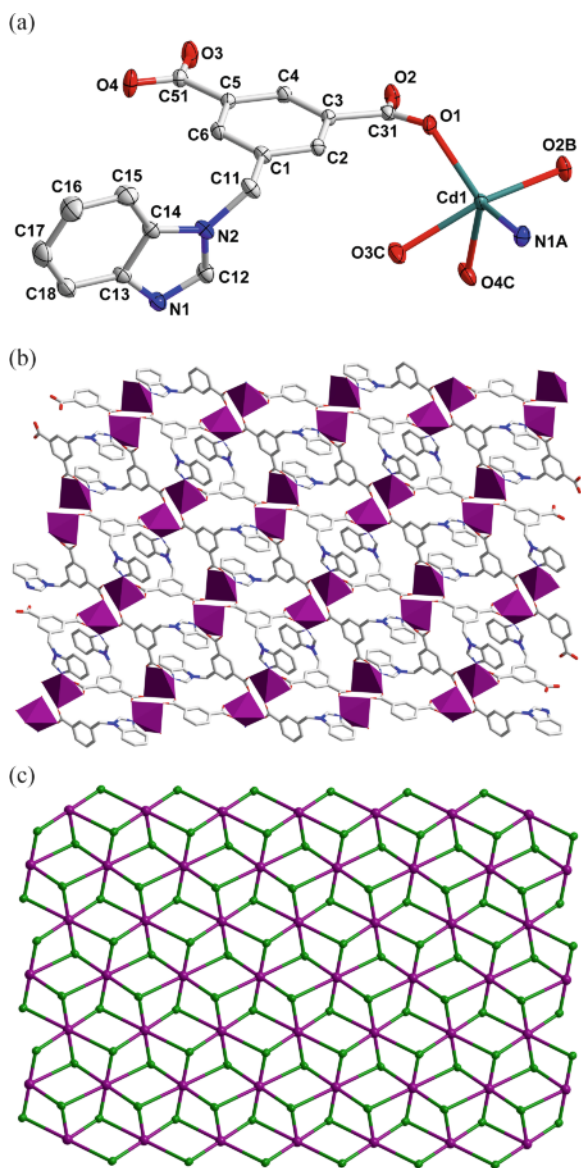


Fig. 1 (color online). (a) The coordination environment of the Cd atoms in **1** with ellipsoids drawn at the 30% probability level. The hydrogen atoms are omitted for clarity. (b) View of the 2D network of **1**. (c) Schematic representation of the binodal (3,6)-connected 2D network of **1**.

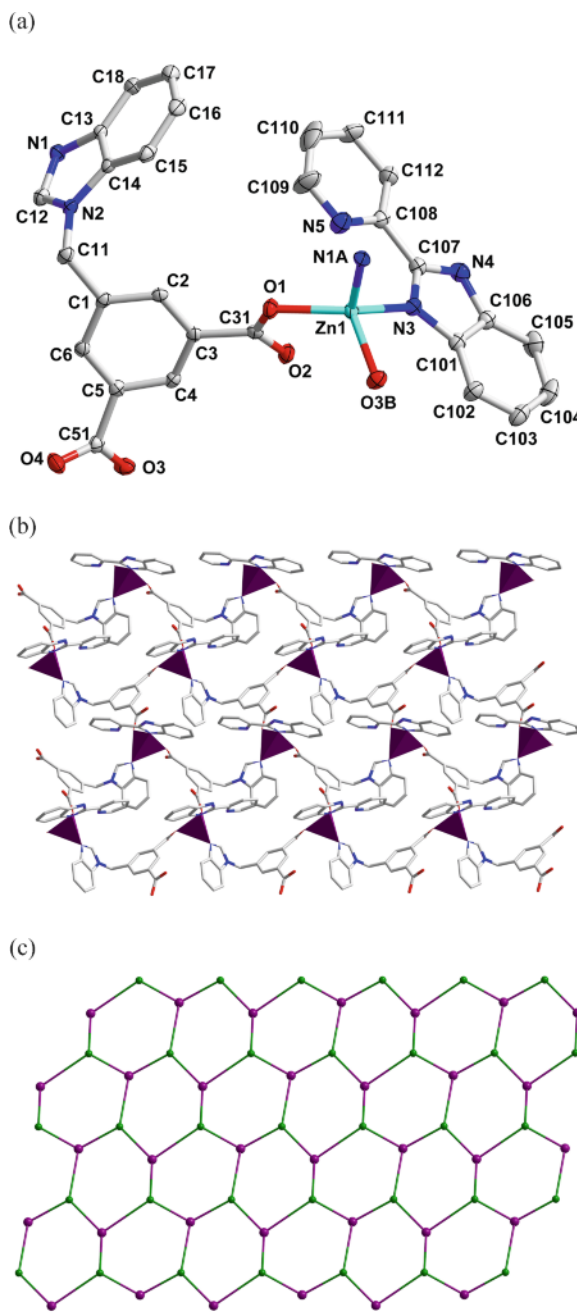


Fig. 2 (color online). (a) The coordination environment of the Zn atoms in **3** with ellipsoids drawn at the 30% probability level. The hydrogen atoms are omitted for clarity. (b) View of the 2D network of **3**. (c) Schematic representation of the uninodal 3-connected 2D network of **3**.

### Coordination modes of the $L^{2-}$ ligand and structural comparison of the complexes

The previously reported complexes with the  $L^{2-}$  ligand, [Co(L)] and [Mn(L)], show similar 2D **kgd** network structures, and the metal coordination numbers are five. Different from the [Zn(L)], [Cd(L)], [Co(L)], and [Mn(L)] complexes, the [Cu(L)] and [Cu<sub>2</sub>(L)(dpe)<sub>0.5</sub>]·2.5H<sub>2</sub>O complexes show a 2-fold interpenetrated 2D **hcb** network and a double-stranded chain structure, respectively. In the presence of pybim as auxiliary ligand, complexes [Co(L)(pybim)]·H<sub>2</sub>O, [Mn(L)(pybim)] and [Zn(L)(pybim)] were obtained. Among them, the Co(II) complex has a 1D structure, and the Mn(II) and Zn(II) complexes show similar 2D structures except for some bond length and angle differences.

### PXRD, IR, and thermal stabilities of complexes 1–3

The phase purity of **1–3** could be proven by powder X-ray diffraction (PXRD) analyses. As shown in Fig. 3, each pattern of the bulk sample was in agreement with the pattern simulated from the corresponding single-crystal data.

The absence of IR bands between 1680 and 1760  $\text{cm}^{-1}$  indicates complete deprotonation of the carboxylic groups of H<sub>2</sub>L. Characteristic bands of carboxylate asymmetric stretches are at 1613 and 1557  $\text{cm}^{-1}$  for **1**, 1625 and 1569  $\text{cm}^{-1}$  for **2**, and 1612 and 1591  $\text{cm}^{-1}$  for **3**. Characteristic bands of carboxylate symmetric stretches appear at 1507 and

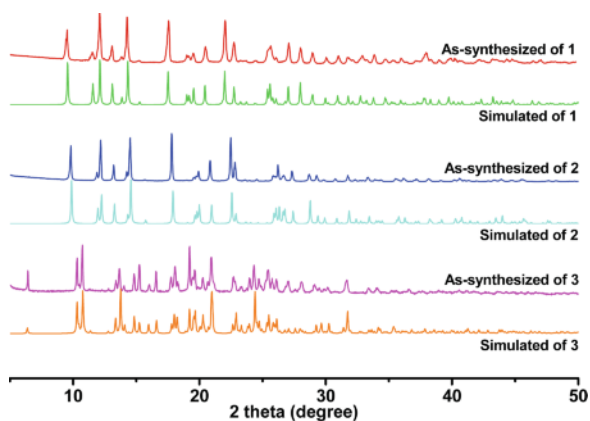


Fig. 3 (color online). The powder X-ray diffraction (PXRD) patterns of complexes **1–3**.

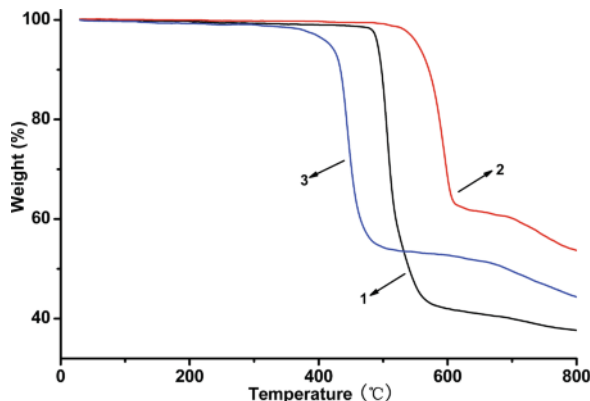


Fig. 4 (color online). TGA curves of complexes **1–3**.

1451  $\text{cm}^{-1}$  for **1**, 1509 and 1453  $\text{cm}^{-1}$  for **2**, and 1501 and 1459  $\text{cm}^{-1}$  for **3**.

To estimate the thermal stability of **1–3**, thermogravimetric analyses (TGA) were carried out under N<sub>2</sub> atmosphere with a heating rate of 10  $^{\circ}\text{C min}^{-1}$ . The TGA curves were recorded from 30 to 800  $^{\circ}\text{C}$ . As shown in Fig. 4, no obvious weight loss can be observed prior to the decomposition of the frameworks starting at 470  $^{\circ}\text{C}$  for **1**, at 524  $^{\circ}\text{C}$  for **2**, and at 400  $^{\circ}\text{C}$  for **3**, which further confirms that no solvent is contained in the structures.

### Luminescence properties

The luminescence properties of complexes with  $d^{10}$  metal centers such as Cd(II) and Zn(II) are of interest for their potential applications as photoactive materials [28–31]. Therefore, the luminescence properties of **1–3**, as well as of the free H<sub>2</sub>L ligand, were investigated in the solid state at room temperature. As shown in Fig. 5, intense bands were observed at 407 nm ( $\lambda_{\text{ex}} = 345$  nm) for **1**, 421 nm ( $\lambda_{\text{ex}} = 344$  nm) for **2**, 404 nm ( $\lambda_{\text{ex}} = 340$  nm) for **3**, and 396 nm ( $\lambda_{\text{ex}} = 338$  nm) for the H<sub>2</sub>L ligand. As for the origin of fluorescence of the complexes, it may be assigned to intra-ligand transitions of the coordinated  $L^{2-}$  ligands, since a similar emission can be observed for the free H<sub>2</sub>L ligand [32–34]. The observed red shifts of the emission maximum for the complexes vs. the H<sub>2</sub>L ligand originate from the coordination interactions [35, 36].

The emission decay lifetimes of complexes **1–3** were measured on an FLS920 spectrofluorimeter under ambient temperature and were analyzed with two

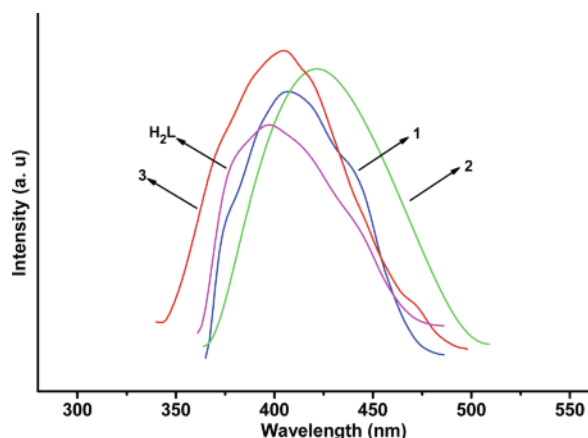


Fig. 5 (color online). Emission spectra of **1–3** and of  $H_2L$  in the solid state at room temperature.

exponentials functions  $f(t)$  [37, 38]:

$$f(t) = A + B_1 \exp(-t/\tau_1) + B_2 \exp(-t/\tau_2) \quad (1)$$

$B_1$  and  $B_2$  are the decay amplitudes,  $A$  is a constant, and  $\tau_1$  and  $\tau_2$  are the time constants of the decay  $i$ . As a result, the decay lifetimes are  $\tau_1 = 2.644 \mu\text{s}$  and  $\tau_2 = 26.16 \mu\text{s}$  ( $\chi^2 = 1.255$ ) for **1**,  $\tau_1 = 2.393 \mu\text{s}$  and  $\tau_2 = 22.74 \mu\text{s}$  ( $\chi^2 = 1.257$ ) for **2**, and  $\tau_1 = 2.446 \mu\text{s}$  and  $\tau_2 = 14.76 \mu\text{s}$  ( $\chi^2 = 1.287$ ) for **3**. The average decay times ( $\tau_{\text{av}}$ ) were calculated using the following formula:

$$\tau_{\text{av}} = \frac{B_1 \tau_1^2 + B_2 \tau_2^2}{B_1 \tau_1 + B_2 \tau_2} \quad (2)$$

and found to be about 21.81, 18.01, and 12.82  $\mu\text{s}$ , respectively. It is noteworthy that the decay lifetimes become shorter from **1** to **3**. Different decay lifetimes of **1** and **2** were observed in spite of the isostructural relation implying that the metal centers have an influence on the photoluminescence. The difference of decay lifetimes in structurally different zinc complexes **2** and **3** may be attributed to different molecular rigidity [39–41].

## Conclusion

The 5-(benzimidazol-1-ylmethyl)isophthalate ligand ( $L^{2-}$ ) was employed as an organic building block with variable coordination modes. Hydrothermal reactions of  $H_2L$  with Cd(II) and Zn(II) salts have pro-

vided the three new complexes [Cd(L)] (**1**), [Zn(L)] (**2**) and [Zn(L)(pybim)] (**3**) [pybim = 2-(pyridin-2-yl)-1*H*-benzimidazole]. Complexes **1** and **2** are isostructural and exhibit binodal (3,6)-connected 2D **kgd** network structures with  $(4^3)_2(4^6.6^6.8^3)$  topology; **3** consists of an uninodal 3-connected 2D ( $6^3$ ) **hcb** network. The results show that auxiliary ligands can influence the coordination modes of the ligand and the structures of the resulting complexes. As expected, the  $d^{10}$  metal complexes exhibit strong luminescence emission.

## Experimental Section

All commercially available chemicals were of reagent grade and used as received without further purification. The  $H_2L$  ligand was synthesized *via* the experimental procedure reported in the literature [42, 43]. Elemental analyses of C, H, and N were carried out on a Perkin-Elmer 240C elemental analyzer. Infrared spectra (IR) were recorded on a Bruker Vector22 FT-IR spectrophotometer by using KBr pellets. Thermogravimetric analysis (TGA) was performed on a simultaneous SDT 2960 thermal analyzer under nitrogen atmosphere with a heating rate of  $10^\circ\text{C min}^{-1}$ . Powder X-ray diffraction (PXRD) patterns were measured on a Shimadzu XRD-6000 X-ray diffractometer with  $\text{CuK}\alpha$  ( $\lambda = 1.5418 \text{ \AA}$ ) radiation at room temperature. The luminescence spectra for the powdered solid samples were measured on an Aminco Bowman Series 2 spectrofluorometer with a xenon arc lamp as the light source. In the measurements of emission and excitation spectra the pass width was 5 nm, and all measurements were carried out under the same experimental conditions.

### Syntheses

For a better conversion of the  $H_2L$  ligand, the metal salts were used in excess to synthesize the complexes **1–3**.

#### Preparation of [Cd(L)] (**1**)

The reaction mixture of  $\text{Cd}(\text{NO}_3)_2 \cdot 4\text{H}_2\text{O}$  (92.7 mg, 0.3 mmol),  $H_2L$  (29.6 mg, 0.1 mmol) and KOH (11.2 mg, 0.2 mmol) in 12 mL  $\text{H}_2\text{O}$  was sealed in a 16 mL Teflon-lined stainless-steel container and heated at  $180^\circ\text{C}$  for 72 h. Then the oven was shut off and cooled down naturally to ambient temperature. After cooling, colorless plates of **1** were obtained with an approximate yield of 20% based on  $H_2L$ . –  $\text{C}_{16}\text{H}_{10}\text{N}_2\text{O}_4\text{Cd}$  (406.67): calcd. C 47.25, H 2.48, N 6.89%; found C 47.51, H 2.19, N 6.62%. – IR (KBr pellet,  $\text{cm}^{-1}$ ):  $\nu = 1613$  (s), 1557 (s), 1507 (s), 1451 (s), 1375 (s), 1294 (w), 1264 (w), 1244 (w), 1183 (w), 1112 (m), 1087 (m), 970 (w),

	<b>1</b>	<b>2</b>	<b>3</b>
Formula	C <sub>16</sub> H <sub>10</sub> N <sub>2</sub> O <sub>4</sub> Cd	C <sub>16</sub> H <sub>10</sub> N <sub>2</sub> O <sub>4</sub> Zn	C <sub>28</sub> H <sub>19</sub> N <sub>5</sub> O <sub>4</sub> Zn
<i>M<sub>r</sub></i>	406.66	359.63	554.85
Crystal size, mm <sup>3</sup>	0.30 × 0.30 × 0.10	0.30 × 0.06 × 0.06	0.20 × 0.20 × 0.20
Crystal system	monoclinic	monoclinic	monoclinic
Space group	<i>P</i> 2 <sub>1</sub> / <i>c</i>	<i>P</i> 2 <sub>1</sub> / <i>c</i>	<i>P</i> 2 <sub>1</sub> / <i>c</i>
<i>a</i> , Å	8.300(2)	8.2704(13)	15.0937(14)
<i>b</i> , Å	11.597(3)	11.2494(18)	10.6709(9)
<i>c</i> , Å	17.395(4)	16.9383(19)	15.6868(14)
β, deg	118.500(9)	119.227(5)	113.477(2)
<i>V</i> , Å <sup>3</sup>	1471.5(6)	1375.3(3)	2317.4(4)
<i>Z</i>	4	4	4
<i>D</i> <sub>calcd.</sub> , g cm <sup>-3</sup>	1.84	1.74	1.59
μ (MoKα), cm <sup>-1</sup>	1.5	1.8	1.1
<i>F</i> (000), e	800	728	1136
<i>hkl</i> range	-6 → +10 -14 → +15 -22 → +21	-4 → +9 ±13 ±20	-19 → +18 -12 → +14 ±20
θ <sub>max</sub> , deg	2.20–27.73	2.28–25.00	2.38–28.00
Refl. total / unique / <i>R</i> <sub>int</sub>	8899 / 3386 / 0.038	6703 / 2418 / 0.039	14321 / 5513 / 0.076
Param. refined	208	208	331
<i>R</i> ( <i>F</i> ) <sup>a</sup> / <i>wR</i> ( <i>F</i> <sup>2</sup> ) <sup>b</sup> (all refls.)	0.0313 / 0.0543	0.0926 / 0.1763	0.1072 / 0.1261
GoF ( <i>F</i> <sup>2</sup> ) <sup>c</sup>	0.949	1.400	0.943
Δρ <sub>fin</sub> (max/min), e Å <sup>-3</sup>	0.49 / -0.47	0.77 / -1.15	0.58 / -0.39

Table 1. Crystal structure data for **1–3**.

<sup>a</sup>  $R = \sum ||F_o| - |F_c|| / \sum |F_o|$ ; <sup>b</sup>  $wR = [\sum w(F_o^2 - F_c^2)^2 / \sum w(F_o^2)^2]^{1/2}$ ,  $w = [\sigma^2(F_o^2) + (AP)^2 + BP]^{-1}$ , where  $P = (\text{Max}(F_o^2, 0) + 2F_c^2) / 3$ ; <sup>c</sup>  $\text{GoF} = [\sum w(F_o^2 - F_c^2)^2 / (n_{\text{obs}} - n_{\text{param}})]^{1/2}$ .

[Cd(L)] ( <b>1</b> )			
Cd(1)–O(1)	2.2191(17)	Cd(1)–O(3)#1	2.3211(18)
Cd(1)–O(4)#1	2.3052(19)	Cd(1)–O(2)#2	2.1979(16)
Cd(1)–N(1)#3	2.224(2)		
O(1)–Cd(1)–O(3)#1	88.60(6)	O(1)–Cd(1)–O(4)#1	130.56(6)
O(1)–Cd(1)–O(2)#2	104.33(7)	O(1)–Cd(1)–N(1)#3	112.22(7)
O(3)#1–Cd(1)–O(4)#1	56.31(6)	O(2)#2–Cd(1)–O(3)#1	156.27(7)
O(3)#1–Cd(1)–N(1)#3	104.23(8)	O(2)#2–Cd(1)–O(4)#1	101.02(7)
O(4)#1–Cd(1)–N(1)#3	109.75(8)	O(2)#2–Cd(1)–N(1)#3	89.41(7)
[Zn(L)] ( <b>2</b> )			
Zn(1)–O(4)	1.989(5)	Zn(1)–O(1)#1	2.040(7)
Zn(1)–O(2)#1	2.290(7)	Zn(1)–O(3)#2	2.000(5)
Zn(1)–N(2)#3	2.012(7)		
O(1)#1–Zn(1)–O(4)	127.9(3)	O(2)#1–Zn(1)–O(4)	86.8(2)
O(3)#2–Zn(1)–O(4)	104.5(2)	O(4)–Zn(1)–N(2)#3	111.7(3)
O(1)#1–Zn(1)–O(2)#1	59.9(2)	O(1)#1–Zn(1)–O(3)#2	98.8(2)
O(1)#1–Zn(1)–N(2)#3	112.2(3)	O(2)#1–Zn(1)–O(3)#2	158.0(2)
O(2)#1–Zn(1)–N(2)#3	99.1(3)	O(3)#2–Zn(1)–N(2)#3	94.2(3)
[Zn(L)(pybim)] ( <b>3</b> )			
Zn(1)–O(1)	1.983(2)	Zn(1)–N(3)	2.059(3)
Zn(1)–N(1)#1	2.036(3)	Zn(1)–O(3)#2	1.994(3)
O(1)–Zn(1)–N(3)	133.35(12)	O(1)–Zn(1)–N(1)#1	99.81(12)
O(1)–Zn(1)–O(3)#2	111.29(11)	N(1)#1–Zn(1)–N(3)	113.33(12)
O(3)#2–Zn(1)–N(3)	94.91(12)	O(3)#2–Zn(1)–N(1)#1	99.83(12)

Table 2. Selected bond lengths (Å) and angles (deg) for complexes **1–3**<sup>a</sup>.

<sup>a</sup> Symmetry transformations used to generate equivalent atoms: For **1**, #1 1 - *x*, 1/2 + *y*, 3/2 - *z*; #2 1 - *x*, -*y*, 1 - *z*; #3 *x*, 1/2 - *y*, -1/2 + *z*; for **2**, #1 1 - *x*, 1/2 + *y*, 1/2 - *z*; #2 -*x*, -*y*, -*z*; #3 -1 + *x*, 1/2 - *y*, -1/2 + *z*; for **3**, #1 *x*, 3/2 - *y*, -1/2 + *z*; #2 *x*, 5/2 - *y*, -1/2 + *z*.



915 (w), 844 (w), 809 (w), 779 (m), 763 (s), 723 (s), 647 (w), 622 (w), 586 (w).

#### Preparation of [Zn(L)] (2)

Complex **2** was synthesized by the same hydrothermal procedure used for **1**, except that Zn(NO<sub>3</sub>)<sub>2</sub>·6H<sub>2</sub>O (89.1 mg, 0.3 mmol) was used instead of Cd(NO<sub>3</sub>)<sub>2</sub>·4H<sub>2</sub>O. Colorless needles of **2** were obtained with an approximate yield of 20% based on H<sub>2</sub>L. – C<sub>16</sub>H<sub>10</sub>N<sub>2</sub>O<sub>4</sub>Zn (359.67): calcd. C 53.43, H 2.80, N 7.79%; found C 53.71, H 2.52, N 7.59%. – IR (KBr pellet, cm<sup>-1</sup>): ν = 1625 (s), 1569 (s), 1509 (s), 1453 (s), 1377 (s), 1301 (m), 1261 (w), 1241 (m), 1185 (s), 1134 (w), 1104 (w), 973 (w), 922 (m), 866 (w), 806 (m), 775 (s), 760 (s), 740 (s), 725 (s), 679 (w), 643 (w), 588 (m), 537 (w).

#### Preparation of [Zn(L)(pybim)] (3)

Complex **3** was obtained under the same reaction condition as those for the preparation of **2** except that pybim (19.5 mg, 0.1 mmol) was also introduced. Colorless block-shaped crystals of **3** were obtained with an approximate yield of 20% based on H<sub>2</sub>L. – C<sub>28</sub>H<sub>19</sub>N<sub>5</sub>O<sub>4</sub>Zn (554.89): calcd. C 60.61, H 3.45, N 12.62%; found C 60.89, H 3.42, N 12.39%. – IR (KBr pellet, cm<sup>-1</sup>): ν = 1612 (s), 1591 (s), 1529 (s), 1501 (m), 1459 (s), 1416 (s), 1380 (m), 1349 (s), 1286 (m), 1231 (m), 1198 (w), 1143 (w), 971 (m), 802 (w), 755 (s), 708 (m), 690 (m), 567 (s).

#### X-Ray structure determinations

The crystallographic data collections for complexes **1–3** were carried out on a Bruker Smart Apex CCD area detector diffractometer using graphite-monochromatized MoK<sub>α</sub> radiation (λ = 0.71073 Å) at 293(2) K. The diffraction data were integrated by using the program SAINT [44], which was also used for the intensity corrections for Lorentz and polarization effects. Semi-empirical absorption corrections were applied using the program SADABS [45]. The structures of **1–3** were solved by Direct Methods, and all non-hydrogen atoms were refined anisotropically on F<sup>2</sup> by the full-matrix least-squares technique using the SHELXL-97 crystallographic software package [46]. In **1–3**, all hydrogen atoms at C atoms were generated geometrically; the hydrogen atoms at N4 of **3** could be found at a reasonable position in the difference Fourier maps and were located as such. The details of crystal parameters, data collection, and refinements are summarized in Table 1; the selected bond lengths and angles are listed in Table 2.

CCDC 917922–917924 contain the supplementary crystallographic data for this paper. These data can be obtained free of charge from The Cambridge Crystallographic Data Centre via [www.ccdc.cam.ac.uk/data\\_request/cif](http://www.ccdc.cam.ac.uk/data_request/cif).

#### Acknowledgement

The authors gratefully acknowledge Huaian Administration of Science & Technology of Jiangsu Province of China (HAG2012022) for financial support of this work.

- [1] Y. Z. Zheng, M. L. Tong, W. Xue, W. X. Zhang, X. M. Chen, F. Grandjean, G. J. Long, *Angew. Chem. Int. Ed.* **2007**, *46*, 6076–6080.
- [2] T. Uemura, Y. Ono, Y. Hijikata, S. Kitagawa, *J. Am. Chem. Soc.* **2010**, *132*, 4917–4924.
- [3] C. Y. Chen, J. Peng, Y. Shen, D. Chen, H. Q. Zhang, C. L. Meng, *Z. Naturforsch.* **2011**, *66b*, 43–48.
- [4] G. C. Liu, J. X. Zhang, X. L. Wang, H. Y. Lin, A. X. Tian, Y. F. Wang, *Z. Naturforsch.* **2011**, *66b*, 125–132.
- [5] S. R. Batten, *J. Solid State Chem.* **2005**, *178*, 2475–2479.
- [6] L. Carlucci, G. Ciani, D. M. Proserpio, S. Rizzato, *Chem. Commun.* **2001**, 1198–1199.
- [7] S. T. Zheng, G. Y. Yang, *Dalton Trans.* **2010**, *39*, 700–703.
- [8] J. Zhang, S. M. Chen, H. Valle, M. Wong, C. Austria, M. Cruz, X. H. Bu, *J. Am. Chem. Soc.* **2007**, *129*, 14168–14169.
- [9] B. Zhao, X. Y. Chen, P. Cheng, D. Z. Liao, S. P. Yan, Z. H. Jiang, *J. Am. Chem. Soc.* **2004**, *126*, 15394–15395.
- [10] H. W. Kuai, X. C. Cheng, X. H. Zhu, *Inorg. Chem. Commun.* **2012**, *25*, 43–47.
- [11] J. Zhang, J. Ensling, V. Ksenofontov, P. Gütllich, A. J. Epstein, J. S. Miller, *Angew. Chem., Int. Ed. Engl.* **1998**, *37*, 657–660.
- [12] K. R. Dunbar, *Angew. Chem., Int. Ed. Engl.* **1996**, *35*, 1659–1661.
- [13] H. Zhao, R. A. Heintz, R. D. Rogers, K. R. Dunbar, *J. Am. Chem. Soc.* **1996**, *118*, 12844–12845.
- [14] W. W. Zhou, J. T. Chen, G. Xu, M. S. Wang, J. P. Zou, X. F. Long, G. J. Wang, G. C. Guo, J. S. Huang, *Chem. Commun.* **2008**, 2762–2764.
- [15] G. Z. Liu, S. H. Li, L. Y. Wang, *CrystEngComm* **2012**, *14*, 880–889.
- [16] G. X. Liu, Y. Q. Huang, Q. Chu, T. A. Okamura, W. Y. Sun, H. Liang, N. Ueyama, *Cryst. Growth Des.* **2008**, *8*, 3233–3245.

- [17] R. Cao, D. Sun, Y. Liang, M. Hong, K. Tatsumi, Q. Shi, *Inorg. Chem.* **2002**, *41*, 2087–2094.
- [18] S. S. Chen, G. C. Lv, J. Fan, T. A. Okamura, M. Chen, W. Y. Sun, *Cryst. Growth Des.* **2011**, *11*, 1082–1090.
- [19] Z. Su, J. Fan, M. Chen, T. A. Okamura, W. Y. Sun, *Cryst. Growth Des.* **2011**, *11*, 1159–1169.
- [20] Z. Su, S. S. Chen, J. Fan, M. S. Chen, Y. Zhao, W. Y. Sun, *Cryst. Growth Des.* **2010**, *10*, 3675–3684.
- [21] H. W. Kuai, X. C. Cheng, X. H. Zhu, *J. Coord. Chem.* **2013**, *66*, 28–41.
- [22] M. Chen, Z. S. Bai, Q. Liu, T. A. Okamura, Y. Lu, W. Y. Sun, *CrystEngComm* **2012**, *14*, 8642–8648.
- [23] M. Chen, Y. Lu, J. Fan, G. C. Lv, Y. Zhao, Y. Zhang, W. Y. Sun, *CrystEngComm* **2012**, *14*, 2015–2023.
- [24] B. Zhao, L. Yi, Y. Dai, X. Y. Chen, P. Cheng, D. Z. Liao, S. P. Yan, Z. H. Jiang, *Inorg. Chem.* **2005**, *44*, 911–920.
- [25] H. W. Kuai, T. A. Okamura, W. Y. Sun, *J. Coord. Chem.* **2012**, *65*, 3147–3159.
- [26] X. C. Cheng, H. W. Kuai, *Z. Naturforsch.* **2012**, *67b*, 1255–1262.
- [27] V. A. Blatov, *IUCr CompComm Newsletter* **2006**, *7*, 4–38.
- [28] H. W. Kuai, X. C. Cheng, X. H. Zhu, *Polyhedron* **2013**, *50*, 390–397.
- [29] Y. B. Dong, P. Wang, R. Q. Huang, M. D. Smith, *Inorg. Chem.* **2004**, *43*, 4727–4739.
- [30] D. M. Ciurtin, N. G. Pschirer, M. D. Smith, U. H. F. Bunz, H. C. zur Loye, *Chem. Mater.* **2001**, *13*, 2743–2745.
- [31] H. W. Kuai, X. C. Cheng, X. H. Zhu, *Polyhedron* **2013**, *53*, 113–121.
- [32] L. Y. Xin, G. Z. Liu, X. L. Li, L. Y. Wang, *Cryst. Growth Des.* **2012**, *12*, 147–157.
- [33] B. Valeur, *Molecular Fluorescence: Principles and Applications*, Wiley-VCH, Weinheim, **2002**.
- [34] Y. Q. Huang, B. Ding, H. B. Song, B. Zhao, P. Ren, P. Cheng, H. G. Wang, D. Z. Liao, S. P. Yan, *Chem. Commun.* **2006**, 4906–4908.
- [35] X. L. Wang, Y. F. Bi, G. C. Liu, H. Y. Lin, T. L. Hu, X. H. Bu, *CrystEngComm* **2008**, *10*, 349–356.
- [36] L. Zhang, Z. J. Li, Q. P. Lin, Y. Y. Qin, J. Zhang, P. X. Yin, J. K. Cheng, Y. G. Yao, *Inorg. Chem.* **2009**, *48*, 6517–6525.
- [37] T. D. Pasatoiu, C. Tiseanu, A. M. Madalan, B. Jurca, C. Duhayon, J. P. Sutter, M. Andruh, *Inorg. Chem.* **2011**, *50*, 5879–5889.
- [38] Z. Y. Li, J. W. Dai, N. Wang, H. H. Qiu, S. T. Yue, Y. L. Liu, *Cryst. Growth Des.* **2010**, *10*, 2746–2751.
- [39] J. L. Song, C. Lei, J. G. Mao, *Inorg. Chem.* **2004**, *43*, 5630–5634.
- [40] W. T. Chen, S. Fukuzumi, *Inorg. Chem.* **2009**, *48*, 3800–3807.
- [41] B. L. Chen, L. B. Wang, F. Zapata, G. D. Qian, E. M. Lobkovsky, *J. Am. Chem. Soc.* **2008**, *130*, 6718–6719.
- [42] H. W. Kuai, J. Fan, Q. Liu, W. Y. Sun, *CrystEngComm* **2012**, *14*, 3708–3716.
- [43] H. W. Kuai, X. C. Cheng, X. H. Zhu, *J. Coord. Chem.* **2011**, *64*, 1636–1644.
- [44] SAINT, Program for Data Extraction and Reduction, Bruker Analytical X-ray Instruments Inc., Madison, Wisconsin (USA) **2001**.
- [45] G. M. Sheldrick, SADABS, Program for Empirical Absorption Correction of Area Detector Data, University of Göttingen, Göttingen (Germany) and Bruker Analytical X-ray Instruments Inc., Madison, Wisconsin (USA) **2002**.
- [46] G. M. Sheldrick, *Acta Crystallogr.* **2008**, *A64*, 112–122.